Journal of Materials, Processing and Design (2023)
Clausius Scientific Press, Canada

DOI: 10.23977/jmpd.2023.070204
ISSN 2516-0923 Vol. 7 Num. 2

Graphene-Based Metal Oxide Composites for Lithium-ion Batteries

Hang Yin

School of Chemical Engineering & Pharmacy, Wuhan Institute of Technology, Wuhan, 430205, Hubei, China

Keywords: Lithium-ion battery; Graphene; Metal oxide; MOF

Abstract: Lithium-ion batteries have attracted widespread public attention because of their excellent energy density and extremely long cycle stability. Metal oxide has been widely used in lithium ion batteries as high-capacity anode materials. However, due to the serious volume expansion effect of metal oxide in the process of lithium removal, the cycle stability and multiplier performance of the battery are very poor. The unique structure of two-dimensional materials can give excellent performance to composite materials by improving the electrical performance of lithium metal oxides. In this paper, a flexible nitrogen-doped carbon-coated garnet-like cluster CoOx was designed by calcination in air using a polyaniline-coated metal-organic framework MOF/ GO as a precursor and loaded on a three-dimensional (3D) graphene skeleton composite (NC@CoOx@GF). This MOF extension-transformed anode material is protected by a pomegranate-like NC@CoOx carbon cluster and a robust 3D graphene skeleton, offering promising prospects for high-performance cathode.

1. Introduction

Lithium-ion batteries are considered as energy storage for electric vehicles and short to medium term stationary due to their excellent energy density [1, 2] and extremely long cycle stability as a power source for automobiles and mobile electronics. Lithium ion batteries have attracted a lot of public attention in the past two decades [3, 4], and the demand for better lithium ion batteries is growing. Demand requires constant innovation to improve safety, extend service life, reduce size, reduce weight and reduce cost. However, the theoretical capacity of commercial lithium-ion battery graphite anode is limited (372 mAh g-1), which is difficult to meet the growing demand for power supply. It is imperative to develop alternative anode materials with more efficient and higher capacity [5]. Due to its higher reversible specific capacity, abundant sources and environmental protection, transition metal oxide (TMO) based materials have attracted more and more attention [6]. However, it should be noted that most TMO electrodes still suffer from low conductivity, significant volume exposure effect, and slow reaction kinetics caused by Li+ embedding/deembedding during charge and discharge [7]. In addition, the powder state particles of MO also make it difficult to apply in the field of flexible devices. Therefore, in order to design TMO with metal-organic frame electrodes with high porosity, many efforts have been made to develop electrodes with high conductivity [8], stable structure, and efficient ion transport [9]. For example, a coating with a

carbon conductive structure or a garnet nanostructure [10] is introduced to ensure a close contact between the active substance and the highly conductive component, or a TMO-based composite with a flexible and highly conductive graphene matrix is constructed [11]. However, each of the above specific methods can usually only solve one problem, but it is difficult to deal with another problem [12]. Therefore, there are still major challenges in developing flexible TMO electrodes with layered structures [13].

Herein, flexible nitrogen-doped carbon layer-encapsulated pomegranate-like clusters of CoOx were designed and loaded on a three-dimensional (3D) graphene backbone composite (NC@CoOx@GF) by using a polyaniline-coated metal-organic framework/graphene oxide as a precursor. By in situ polymerization and subsequent calcination in air, the 3D NC@CoOx@GF composites with the dual protection of garnet-like NC@CoOx carbon clusters and a robust 3D graphene backbone offer a promising future for high-performance negative electrodes.

2. Experiment

2.1 Preparation of graphene oxide

The graphene oxide (GO) solution used in this experiment was prepared based on the modified REDOX Hummers method. First, 10 g of 100-mesh graphite sheets and 7.5 g of sodium nitrate were added into a 2L beaker, and then 300 mL of concentrated sulfuric acid was added. The aluminum foil was cut to fit the beaker mouth, and the beaker mouth was covered to prevent ash from entering. After stirring for half an hour, slowly add 40 g potassium permanganate in the stirring state. Keep stirring for another two days and let it sit sealed for a week. Then add 1 L of deionized water and 60 mL of 3% hydrogen peroxide solution in the stirring state, and let it stand after the stirring reaction for 5 hours. Finally, the brown and yellow viscous liquid can be obtained by centrifugation. After dialysis bag for a week, pure GO solution can be obtained. The concentration of GO solution used in this experiment was 4 mg mL-1.

2.2 Preparation route of flexible carbon-nitrogen coated Co oxide/graphene composites

The synthesis of NC@CoOx@GF is shown in Figure 1. The Co-MOF particles are first uniformly anchored to the GO surface by electrostatic and coordination interactions (Co-MOF@GO) [14]. PANI was then coated on Co-MOF@GO surface by in-situ polymerization to form PANI@Co-MOF@GO core-shell structure. After concentration and freeze-drying of the pre-prepared PANI@CoMOF@GO, 3D macropore structure can be obtained, while PANI is carbonized into nitrogen-doped carbon at 350°C. Due to the protective action of PANI, the cyanide organic ligand of Co-MOF is also directly carbonized during this thermal process. At the same time, MOF is crushed and converted into ultra-small CoOx particles and coated with cyanide ligands derived from PANI doped carbon and MOF. Finally, a flexible carbon-nitrogen coated Co oxide/graphene composite with pomegranate cluster structure NC@CoOx@GF was obtained.

2.3 Material structure and morphology test

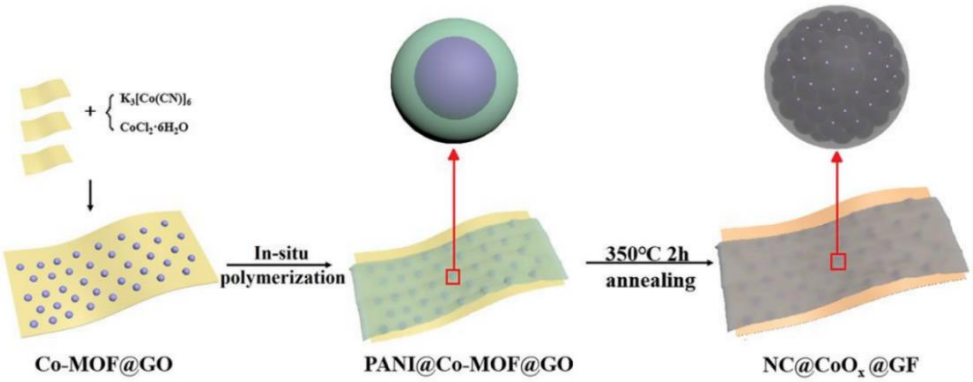

Figure 1: Material preparation process of NC@CoOx@GF

The morphology and structure of the samples were measured by field emission transmission electron microscope (TEM, JEOL JEM-2100F) and scanning electron microscope (SEM, JEOL JSM 7500F). The material generation was tested by X-ray diffraction (XRD, X'Pert PRO MPD) analysis.

2.4 Electrochemical performance test of materials

NC@CoOx@GF, CoOx@GF and NC@GF are directly pressed into thin films. Due to the flexible properties of graphene, they can be directly used as negative electrodes without any adhesive. For NC@CoOx and pure CoOx, adhesive coating assembly is required. The active material powder, carbon black and polyvinylidene fluoride are mixed at a mass ratio of 8:1:1, and the slurry is mixed for 1-3 h. The above slurry is evenly coated on copper foil (99.6%) and then put into vacuum drying oven. After drying, it is cut into rounds by a tablet press and used as negative electrode material for lithium-ion battery assembly.

All charge and discharge tests were carried out by the blue CT2001A test instrument with potential range of 0.01-3.0V. The current density is 100 mA g-1 for the constant current test and 1000 mA g-1 for the long cycle test. The current densities measured by magnification are 100, 200, 400, 800, 1000, 2000, 4000, 6000 and 8000 mA g-1, respectively.

A CHI 760D electrochemical workstation used cyclic voltammetry (CV) to test the electrode performance of the lithium-ion half battery. It is tested according to the connection of working electrode, counter electrode and reference electrode. The CV scanning rate are 0.1, 0.2, 0.5, 1, 2, 5, 10 mV s-1. The sweep voltage range is 0.01-3 V.

3. Results and discussion

3.1 Morphology characterization

The morphology changes of CoOx@GF and NC@CoOx@GF composites before and after heat treatment are shown in Figure 2 and Figure 3. The Co-MOF nanoparticles prepared at CoMOF@GO were generated by the interaction of cobalt ions with cyanide ligands and were uniformly anchored to the GO sheet prior to carbonization (Figure 2a). After 2h calcination in 350℃ air, the organic ligands of Co-MOF nanoparticles are fully decomposed into nitrogenous gas and crushed into a large number of ultrafine CoOx nanoparticles, which are highly crystalline on the graphene surface of CoOx@GF composite (Figure 2b-c, Figure 3c). TEM characterization clearly

showed that Co-MOF particles were successfully coated by PANI layer and formed core-shell structure (Figure 2d). After carbonization, most of the polyaniline is converted into nitrogen-doped carbon layer. Due to the protection of the nitrogen-doped carbon layer derived from polyaniline in the cyanide complex, Co-MOF is decomposed into nitrogen-containing gas and directly carbonized. This phenomenon is similar to the process of chemical vapor deposition, in which the organic ligands of Co-MOF degrade to produce nitrogen-containing gases. Due to the double protection of carbon from the polyaniline and cyanide ligand, the desired pomegranate-like NC@CoOx cluster is formed in the final NC@CoOx@GF composite (Figure 2e-f). High-resolution transmission electron microscopy (HR-TEM) also showed that the (400) surface of Co-MOFs with a lattice of 0.25 nm was confined to nitrogen-doped carbon (Figure 2g). In addition, the element mapping analysis of NC@CoOx@GF also shows the uniform distribution of C, N, O and Co in the composites (Figure 2h-l). It can be seen that C and N components are uniformly distributed on the surface of the composite, while Co and O components are only visible in the clusters, which further indicates that CoOx particles are successfully limited by N-doped carbon. For comparison, the morphologies of NC@CoOx, pure CoOx and NC@GF samples were also standardized by SEM and TEM (Figure 3d-h). NC@CoOx, CoOx particles are coated with solid N-doped carbon layers (Figure 3 d-e). For pure CoOx, the CoOx particles show a porous structure after MOF calcination (Figure 3f-g). At the same time NC@GF shows the macroporous structure.

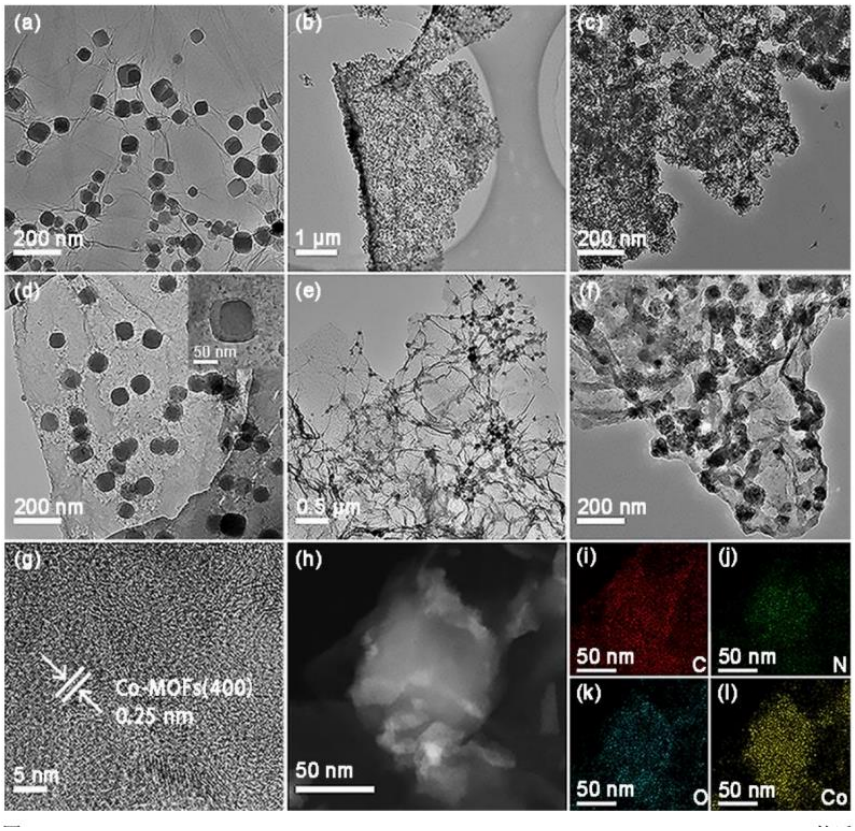

Figure 2: TEM images of (a)Co-MOF@GO, (b, c) CoOx@GF, (d) PANI@Co-MOF@GO, (e-g) NC@CoOx@GF, the scanning TEM images of (h) NC@CoOx@GF, the corresponding elemental mapping images of (i) C, (j) N, (k) O, and (l) Co.

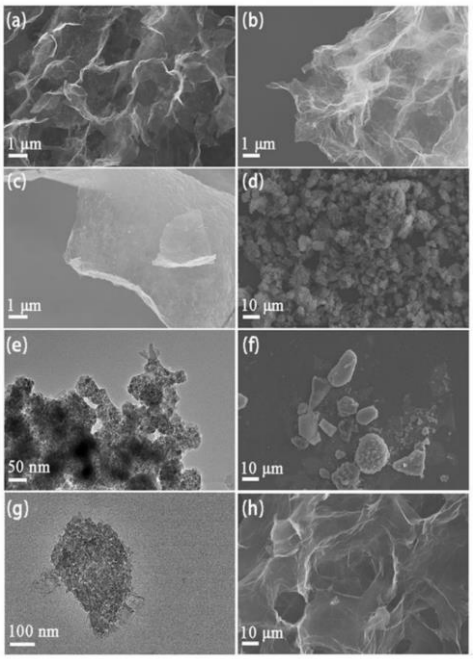

Figure 3: SEM image of (a) PANI@Co-MOF@GO, (b) NC@CoOx@GF, (c) CoOx@GF. SEM image and TEM image of (d-e) NC@CoOx. SEM image (f) and TEM image (g) of pure CoOx. SEM image of (h) NC@GF.

In order to better understand the crystal structure of the composites, NC@CoOx@GF, CoOx@GF, pure CoOx, PANI@Co-MOF@GO, NC@CoOx and NC@GF were characterized by XRD (Figure 4). For PANI@Co-MOF@GO, it shows clear peaks at 17.2 º, 24.5 º, 34.9 º, and 39.4 º Corresponds to the typical Co-MOF (JCPDS#77-1161)[15]. After calcination, for NC@CoOx@GF, it has only a small peak at 17.2 º and a wide peak near 24.5 º, which is attributable to CoOx(JCPDS#77-1161). This result is in good agreement with the HRTEM observation. NC@GF only a wide peak appears near 24.5 º, indicating the presence of an amorphous carbon layer.

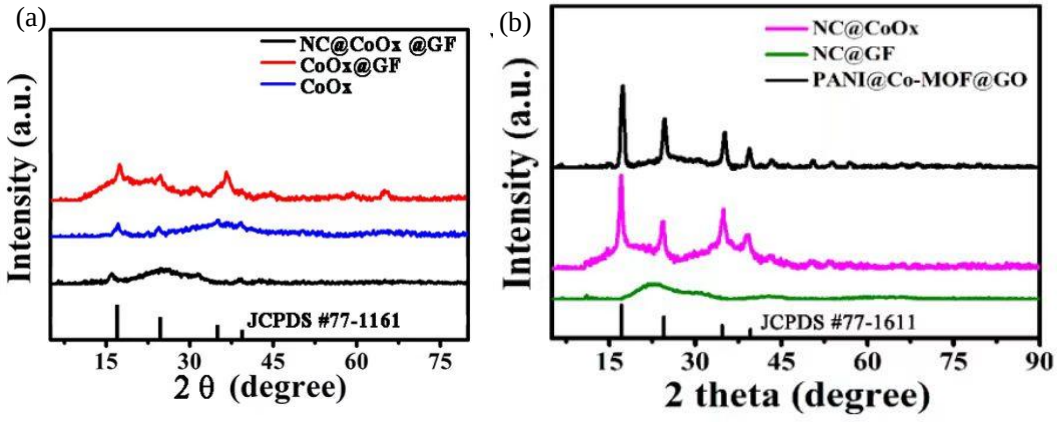

Figure 4: (a) XRD patterns of NC@CoOx@GF, CoOx@GF, CoOx. (b) XRD patterns of NC@CoOx, NC@GF, PANI@Co-MOF@GO

In the electrochemical performance characterization and analysis, CV curves, charge-discharge tests, cross-flow cycle performance tests, rate performance tests, impedance tests, long cycle tests and full battery tests were respectively tested for the main sample and the contrast sample (Figure 5). The detailed properties are analyzed below: Figure 5a illustrates the cyclic voltammetry (CV) of the

flexible binderless NC@CoOx@GF electrode. For the first cathode scan, three clear reduction peaks were observed at 0.5, 0.8, and 1.4V vs. Li/Li+. This is due to the multi-step reduction reaction of CoOx with Li+, the deoxidation of CoOx to cobalt metal, and the irreversible reduction reaction of electrolyte to form the solid electrolyte interface (SEI) film [16]. In subsequent cycles, the three peaks become weaker and move to higher voltages (one at 0.69V, another at 1.38V, and the other disappears) due to intense structural degradation and large volume strains due to lithium embedding/deembedding. For the following anode scan, there are two oxidation peaks (1.03V and 1.37V) in the following anode process. The significant 1.37V peak was attributed to the oxidation of Co to CoOx, while the small but insignificant peak at 1.03V was due to the decomposition of LiF and Li2CO3 in the SEI component. Moreover, the typical charge/discharge curve of NC@CoOx@GF shows a plateau at 0.69-1.38V (Figure 5b), which is completely consistent with the CV test results. Meanwhile, the charge-discharge curve of NC@CoOx@GF in the second cycle is almost consistent with that in the 10th, 50th and 100th cycles, showing excellent electrochemical performance and cycle stability.

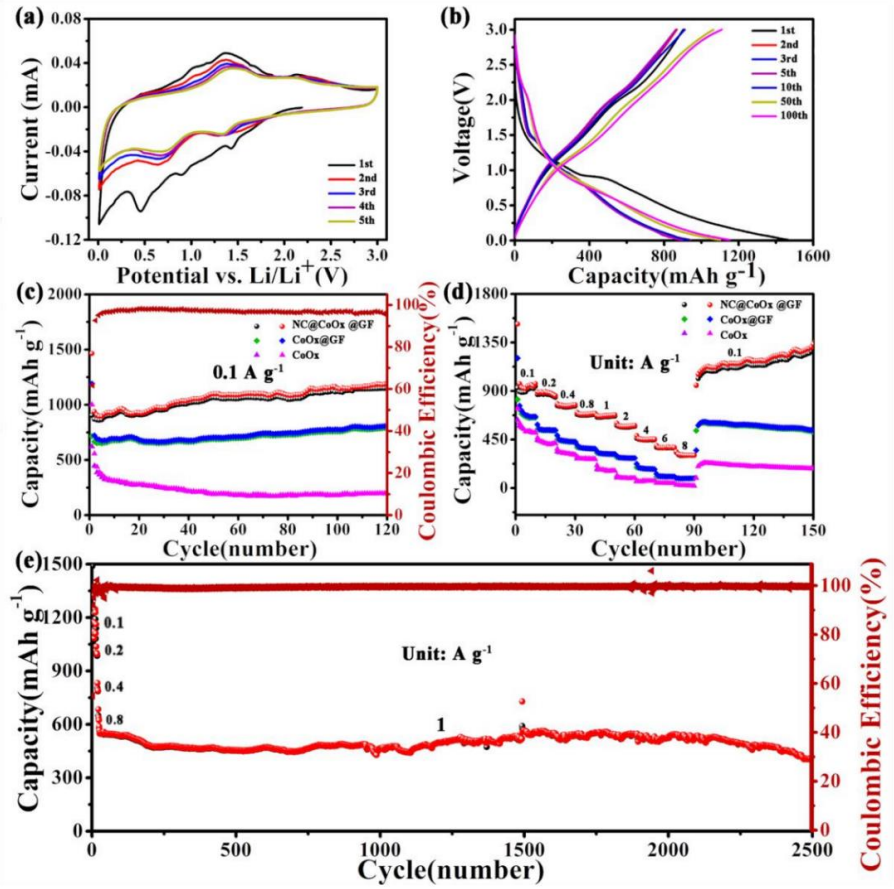

Figure 5: Electrochemical characterizations of NC@CoOx@GF, CoOx@GF, CoOx: (a) CV of NC@CoOx@GF at scan rate of 0.1 mV s-1 ; (b) Charge-discharge curves of NC@CoOx@GF; (c) Cycling capability of NC@CoOx@GF, CoOx@GF, CoOx; (d) Rate capability of NC@CoOx@GF, CoOx@GF, CoOx; (e) Long cycle capability of NC@CoOx@GF.

4. Conclusion

In this paper, cobalt chloride hexahydrate, potassium hexadecyanocobaltate and graphene oxide were combined as raw materials, and aniline hydrochloric acid was added overnight to coat polyaniline. Flexible Co oxide/graphene composites coated with carbon and nitrogen layers were

successfully prepared by in-situ polymerization. Morphologic analysis shows that the pomegranate-like NC@CoOx carbon clusters grow uniformly on the solid 3D graphene skeleton. The nitrogen-doped carbon layer and graphene provide double protection. The crystal structure of the composite was proved by XRD characterization. The electrochemical performance test shows that the pomegranate NC@CoOx cluster can effectively inhibit the volume expansion of CoOx in the charging and discharging process. Meanwhile, a large number of nitrogen-doped carbon from organic ligands around CoOx can act as a multi-micro collector, which is beneficial to electron transmission, thus achieving higher rate performance. The flexible 3D graphene skeleton facilitates the diffusion and transport of Li+ ions, thus achieving ultra-long stability. Obviously, the excellent electrochemical performance of NC@CoOx@GF composite can be attributed to the synergistic effect of pomegranate NC@CoOx cluster and 3D graphene framework. The composite material has great application prospects, especially in the field of new energy conversion and storage, which lays a foundation for the study of high-performance flexible electrodes and two-dimensional materials and metal oxide composite electrodes.

References

[1] Torjesen I. Fossil Fuel Air Pollution Blamed for 1 in 5 Deaths Worldwide. The British Medical Journal, 2021, 372: 406.

[2] Roberts H. M., Shafran R. Reasons to Be Cheerful: The Other Global Crisis. The British Medical Journal, 2021, 370: 2627.

[3] Wang D. G., Qiu T., Guo W. Covalent Organic Framework-based Materials for Energy Applications. Energy & Environmental Science, 2020, 14: 688-728.

[4] Wu F, Maier J, Yu Y. Guidelines and Trends for Next-Generation Rechargeable Lithium and Lithium-ion Batteries. Chemical Society Reviews, 2020, 49(14): 1569-1614.

[5] Wang Z, Zhang X, Liu X, Zhang W, Bakenov Z. Dual-Network Nanoporous NiFe2O4/NiO Composites for High Performance Li-ion Battery Anodes. Chemical Engineering Journal, 2020, 388: 124207.

[6] Gao C, Jiang Z, Wang P, Jensen L R, Yue Y. Optimized Assembling of MOF/SnO2/Graphene Leads to Superior Anode for Lithium Ion Batteries. Nano Energy, 2020, 74: 104868.

[7] Wang F, Feng T, Jin X. Atomic Co/Ni Active Sites Assisted MOF-Derived Rich Nitrogen Doped Carbon Hollow Nanocages for Enhanced Lithium Storage. Chemical Engineering Journal, 2020, 420: 127583.

[8] Zhou T, Shen J, Wang Z, Liu J, Zhu M. Regulating Lithium Nucleation and Deposition via MOF-Derived Co@C-Modified Carbon Cloth for Stable Li Metal Anode. Advanced Functional Materials, 2020, 30(1): 1909159.

[9] Fan M.M., Liao D.K., Aboud M.F., Shakir I., Xu Y.X. A Universal Strategy toward Ultrasmall Hollow Nanostructures with Remarkable Electrochemical Performance. Angewandte Chemie International Edition, 2020, 21: 8247-8254.

[10] Chen Z, An X, Dai L, Xu Y. Holey Graphene-Based Nanocomposites for Efficient Electrochemical Energy Storage. Nano Energy, 2020, 73: 104762.

[11] Luo R, Yu Q, Lu Y, Zhang M, Peng T. 3D Pomegranate-Like TiN@Graphene Composites with Electrochemical Reaction Chambers as Sulfur Hosts for Ultralong-Life LithiumSulfur Batteries. Nanoscale Horizons, 2019, 4(1):531-539.

[12] Zhang C, Nicolosi V. Graphene and MXene-Based Transparent Conductive Electrodes and Supercapacitors. Energy Storage Materials, 2018, 16(4): 102-125.

[13] Xu K, Shen X, Song C, Chen H, Chen Y, Ji Z, Yuan A, Yang X, Kong L. Construction of RGO-Encapsulated Co3O4-CoFe2O4 Composites with A Double-Buffer Structure for HighPerformance Lithium Storage. Small, 2021, 17: 2101080.

[14] Jayakumar A, Antony R P, Wang R, Lee J M. MOF-Derived Hollow Cage NixCo3-xO4 and Their Synergy with Graphene for Outstanding Supercapacitors. Small, 2017, 13: 1603102.

[15] Xiao P T, Bu F X, Zhao R R. Sub-5 nm Ultrasmall Metal-Organic Framework Nanocrystals for Highly Efficient Electrochemical Energy Storage. ACS Nano, 2018, 12(3): 3947-3953.

[16] Huang S, Yang L, Xu G, Wei T, Wei X. Hollow Co3O4@N-doped Carbon Nanocrystals Anchored on Carbon Nanotubes for Freestanding Anode with Superior Li/Na Storage Performance. Chemical Engineering Journal, 2021, 415: 128861.